

Enhancement of Bone Mineralization and Osteoprogenitor Activity by *Berberis vulgaris* L.: Insights into BMP-2 and RANK Pathway Modulation in a Rat Femur Fracture Model

Mejora de la Mineralización Ósea y la Actividad Osteoprogenitora por *Berberis vulgaris* L.: Perspectivas sobre la Modulación de la Vía BMP-2 y RANK en un Modelo de Fractura de Fémur de Rata

Jingjing Bai¹ & Qingfu Liang²

BAI, J. & LIANG, Q. Enhancement of bone mineralization and osteoprogenitor activity by *Berberis vulgaris* L.: Insights into BMP-2 and RANK pathway modulation in a rat femur fracture model. *Int. J. Morphol.*, 43(1):258-268, 2025.

SUMMARY: *Berberis vulgaris* L. (BV) is rich in isoflavonoids and essential minerals that may enhance bone repair by promoting osteoblast differentiation, stimulating osteoprogenitors, and inhibiting osteoclast activity. This study explored the effects of BV extract on bone healing using a femur fracture model in Wistar rats. Eighty rats were divided into eight groups, including a normal control receiving distilled water (DW), a BV-treated group receiving 200 mg/kg of BV daily, a fracture group treated with DW, and fracture groups receiving either 200 or 400 mg/kg of BV daily. Additionally, a fracture group was given Osteocare (OC) syrup, while two combinatory groups received BV with OC syrup. Radiographic assessments of femur fractures and Bone Mineral Density (BMD) were conducted at 30, 60, and 90 days using Dual-energy X-ray absorptiometry (DXA). Serum levels of calcium, phosphorus, and alkaline phosphatase (ALP) were measured, along with calcitonin and parathyroid hormone (PTH) using ELISA kits. Bone tissue was analyzed for p53 gene expression through immunohistochemistry, and osteoprogenitor stimulation was evaluated by measuring OPG, RANK, RANKL, and BMP-2 gene expression. The results indicated that BV supplementation significantly improved BMD and enhanced serum levels of bone formation markers and osteogenesis-related hormones. The study suggests that BV positively influences bone healing through modulation of the OPG/RANK/BMP-2 pathway and may be a promising therapeutic agent for fracture healing and osteoporosis management.

KEY WORDS: Osteogenesis; Bone mineral density; Bone healing; *Berberis vulgaris* L.; Femur fracture.

INTRODUCTION

Bone repair is a complex process governed by numerous cellular and molecular factors, with key influences including age, nutrition, systemic health conditions, lifestyle choices like smoking and alcohol consumption, medication use, and the mechanical stability of the bone (Houschyar *et al.*, 2020). Younger individuals typically experience faster and more complete bone healing due to better bone density and quality, whereas older adults may face slower regeneration and higher risks of complications. Adequate intake of nutrients, particularly calcium and vitamin D, is essential for bone growth and repair (Goodman *et al.*, 2019). Systemic diseases such as diabetes, osteoporosis, and cancer, along with medications like corticosteroids and chemotherapy, significantly impact bone healing. Hormones like calcitonin and parathyroid hormone (PTH) are crucial in maintaining bone homeostasis and facilitating repair by regulating the

osteoblast/osteoclast ratio and promoting the production of matrix vesicles necessary for bone tissue repair and mineralization (Babic Leko *et al.*, 2022; Xie *et al.*, 2020).

Central to the bone repair process is the OPG/RANK/RANKL/BMP-2 signaling pathway, which involves osteoprotegerin (OPG), receptor activator of nuclear factor Kappa-B (RANK), receptor activator of nuclear factor Kappa-B ligand (RANKL), and bone morphogenetic protein-2 (BMP-2). RANKL, produced mainly by osteoblasts, activates osteoclasts to resorb bone, while OPG inhibits this activity by acting as a decoy receptor for RANKL (Zhao *et al.*, 2019; Xue *et al.*, 2021). During repair, RANKL levels initially rise to promote osteoclast activity, which is later countered by increased OPG levels to facilitate bone formation (Tobeiha *et al.*, 2020). BMP-2 supports bone repair

¹ Department of Orthopaedics, Xi'an Hospital of Traditional Chinese Medicine, Xi'an, Shaanxi, People's Republic of China.

² Department of Orthopaedics, Xi'an International Medical Center Hospital, Xi'an, Shaanxi, People's Republic of China.

by promoting osteoblast differentiation and bone matrix production while also stimulating OPG to moderate osteoclast activity. The balance of these interactions is critical, particularly as an elevated RANKL/OPG ratio—common with aging and decreased calcium levels—can lead to impaired bone repair by favoring bone resorption over formation (Lv *et al.*, 2019; Zhang *et al.*, 2022). This pathway is a key therapeutic target in bone repair and regeneration.

Reactive oxygen species (ROS) and inflammatory cytokines such as interleukin-1 (IL-1), interleukin-6 (IL-6), and tumor necrosis factor-alpha (TNF- α) play crucial roles in bone repair, yet their excessive production can be detrimental. During the early stages of bone healing, ROS and cytokines attract immune cells to the injury site, aiding in tissue clearance and promoting angiogenesis. However, as healing progresses, it is essential for the production of these molecules to decrease to allow for osteoblast-driven bone formation (Kobayashi *et al.*, 2015). Disruptions in the balance between ROS and cytokines can impair healing, with excessive ROS leading to increased RANKL expression and bone resorption, while antioxidants help restore the RANKL/OPG balance, promoting bone health. The IL-1 β /BMP-2, IL-6/RANK-L, and TNF- α /OPG pathways are critical in regulating osteoblast and osteoclast activities during bone repair (Azizieh *et al.*, 2019). Pharmacological interventions like Romosozumab, Denosumab, and bisphosphonates target these pathways to enhance bone formation and reduce resorption. Additionally, natural supplements rich in minerals and polyphenols, such as isoflavonoids and flavonoids, can promote osteogenesis by modulating these pathways, often via estrogen receptor-mediated mechanisms (Wu *et al.*, 2023).

Berberis vulgaris L. (BV), a plant rich in berberine, flavonoids, and essential minerals, has demonstrated significant anti-cancer, anti-diabetic, antioxidant, and anti-inflammatory effects (Rahimi *et al.*, 2017). BV's

compounds, including genistein and kaempferol, have been shown to enhance BMP-2 and OPG expression while reducing RANK-L, fostering osteoblast activity and inhibiting osteoclasts (Patidar *et al.*, 2022). This study aims to explore BV's potential in bone healing, particularly in femur fractures, through a comprehensive biochemical, molecular, and histopathological analysis.

MATERIAL AND METHOD

Preparation of BV extract. To prepare the BV extract, 5550 grams of dried BV was ground into a fine powder using a soil grinder (Cat. No. H-4199.5F; Humboldt Company, US). This powder was then mixed with a solvent solution of hexane and methanol (30:70 v/v) and incubated at 34 °C in the dark for 48 h. Following incubation, the mixture was filtered through No. 42 paper filter (Cat. No. 1442-125; Millipore, US) and concentrated using a rotary evaporator (model 9230; Buchi Rotavapor, Switzerland). The final BV extract, yielding 450 g with an extraction efficiency of 8.1 %, was subsequently stored at -4 °C (Shaldoum *et al.*, 2021).

Animal care procedures, group assignments, treatment protocols, experimental design, and research timeline

Rat fracture model and animal care. To induce femur fractures in the rats, a standardized procedure involving sedation and anesthesia was used, administering ketamine at 45 mg/kg and xylazine at 30 mg/kg. The area around the femur, approximately 1 cm below the femoral head, was shaved. A closed fracture was then produced using surgical scissors, following the protocol established by Sun *et al.* (2015), (Fig. 1). Eighty adult Wistar rats, each three months old and weighing approximately 220 \pm 30 g, were housed in propylene cages under controlled conditions: a temperature of 25 \pm 2°C, relative humidity of 50 \pm 3 %, and a 12-h light/dark cycle. The rats were allowed to acclimate to these standard laboratory conditions for 72 h prior to the induction of the closed femur fracture model. They had unrestricted access to clean tap water and standard laboratory rat pellets. The housing and handling of the rats adhered to international standards and ethical guidelines set by the ethics committee of Xi'an International Medical Center Hospital.

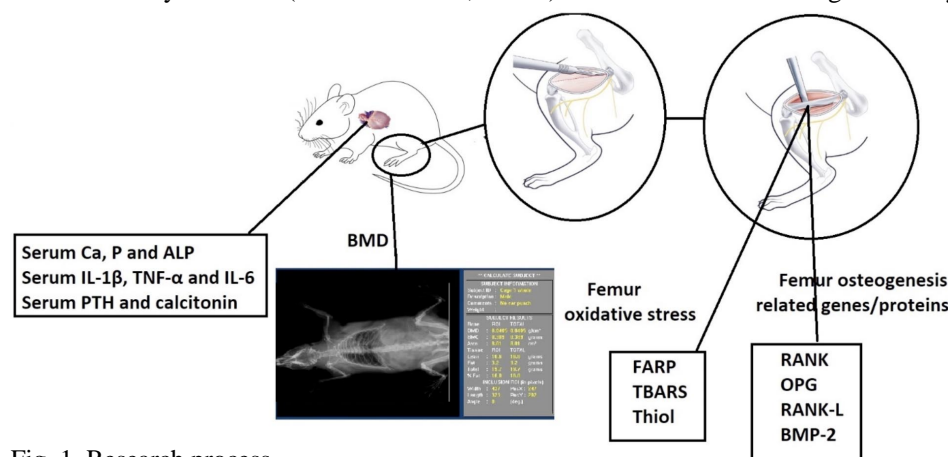


Fig. 1. Research process.

Animal grouping. Following the induction of closed femoral fractures, the rats were randomly assigned to one of eight groups. Over the course of the 90-day study, treatments were administered daily: BV was given at 9:00 am, and osteocalcin (OC) was administered at 3:00 pm. The BV dosage was determined through literature review, a preliminary study, and the LD₅₀ method to ensure both efficacy and safety (Sun *et al.*, 2015; Shaldoum *et al.*, 2021). The treatment groups were as follows:

1. Normal control: 0.5 cc of distilled water (DW) via gavage for 90 days.
2. FX control: 0.5 cc of DW via gavage for 90 days.
3. Normal + 200 BV: 200 mg/kg BV daily via gavage for 90 days.
4. FX + 200 BV: 200 mg/kg BV daily via gavage for 90 days.
5. FX + 400 BV: 400 mg/kg BV daily via gavage for 90 days.
6. FX + OC: 1 mL OC daily via gavage for 90 days.
7. FX + 200 BV + OC: 200 mg/kg BV and 1 mL OC daily via gavage for 90 days.
8. FX + 400 BV + OC: 400 mg/kg BV and 1 mL OC daily via gavage for 90 days.

Acute toxicity test (LD₅₀) for BV. To identify the optimal treatment dose of BV with minimal toxicity, Lork's two-step method was employed. Initially, nine rats were divided into three groups of three (n = 3 per group) and administered doses of 20, 200, and 2000 mg/kg via gavage. Following this, an additional three rats were divided into three separate groups and given doses of 50, 500, and 5000 mg/kg. After a 24-hour observation period, the LD₅₀ of BV was calculated using the formula:

$$LD50=A \times B/2$$

Here, "A" represents the lowest dose at which toxic symptoms (including weight loss, diarrhea, nausea, and skin rashes) or fatalities were observed, while "B" denotes the highest dose at which no toxic symptoms or deaths occurred (John-Africa, 2019). The appropriate dose for the study was then selected based on these results.

Bone densitometry. The rats underwent sedation and anesthesia with ketamine (45 mg/kg) and xylazine (30 mg/kg) to achieve ventral recumbency. Dual-energy X-ray absorptiometry (DXA) scans were conducted on days 0, 30, 60, and 90 of the study using a dedicated DXA scanner. The resulting scans were analyzed with Small Animal Analysis Software (LI-COR Biosciences) to assess bone mineral density and other related parameters (Wong *et al.*, 2018).

Serum concentrations of calcitonin of parathyroid hormone (PTH). On the 91st day, at the conclusion of the study, the rats were euthanized following a pre-anesthesia protocol of 100 mg/kg xylazine (2 %) and an anesthesia protocol of 15 mg/kg ketamine (10 %). Blood was collected directly from the heart, and serum was separated by centrifuging the blood samples at 10,000 g for 15 min. Serum levels of parathyroid hormone (PTH) and calcitonin were assessed using Novus ELISA kits (Novus Biologicals, USA). The assay was conducted according to the manufacturer's instructions. Specifically, 100 µL of each standard, control, and sample was added to 96-well plates. Then, 200 µL of enzyme conjugate was added to each well. After incubating the plates at room temperature for 120 min, the wells were washed three times with 400 µL of washing solution. Subsequently, 200 µL of substrate solution was added, and after a 30-minute incubation, 100 µL of stop solution was introduced. The absorbance was measured at 450 nm using an ELISA reader (Model No. Spectronic 20; Milton Roy Company, Spain) (Zhang *et al.*, 2021).

Serum concentrations of calcium (Ca) and phosphorus (P) levels, and alkaline phosphatase (ALP) activity. The serum was separated by centrifuging the blood at 10,000 g for 20 min. Serum levels of phosphorus (P) and calcium (Ca), along with alkaline phosphatase (ALP) activity, were assessed using Abcam ELISA kits (Abcam, USA). The assays followed the manufacturer's guidelines and protocols, similar to the procedures used for measuring PTH and calcitonin levels (Zhang *et al.*, 2021).

Serum concentrations of tumor necrosis factor-α (TNF-α), interleukin - 1β (IL-1β), and IL-6 levels. Following the separation of serum through centrifugation of blood at 10,000 g for 20 min, levels of IL-1β, IL-6, and TNF-α were quantified using ELISA kits from Abcam (Abcam, USA). These measurements were conducted using a similar procedure to that employed for PTH and calcitonin hormone assays, adhering to the manufacturer's guidelines and protocol (Zhang *et al.*, 2021).

Femur total thiol, lipid peroxidation levels (TBARS), and ferric reducing antioxidant power (FRAP) levels. To assess the total antioxidant capacity of femur tissue using the FRAP method, the femur was first dissected, and a tissue homogenate was prepared. A 200 µL aliquot of this homogenate was then incubated with the FRAP reagent, which consists of 5 mL of 2,4,6-Tripyridyl-S-Triazine (TPTZ), 50 ml of acetate buffer, and 3 mL of ferric chloride solution, at 37 °C for 10 min. The absorbance of the resulting solution was measured at 593 nm using a Stat Fax ELISA reader (Stat Fax, United States), and the total antioxidant capacity was expressed as µmol/mg protein (Shaldoum *et al.*, 2021).

For evaluating lipid peroxidation in femur tissue, the TBARS assay was employed. In this procedure, 100 μ L of the homogenized femur tissue was mixed with a TBARS solution containing 50 μ L of thiobarbituric acid, 2 μ L of butylated hydroxytoluene, and 50 μ L of phosphoric acid, and then incubated at 37 °C for 30 min. The absorbance of the mixture was measured at 532 nm using a Stat Fax ELISA reader (Stat Fax, United States), and the TBARS level was reported as nmol/mg protein (Shaldoum *et al.*, 2021).

To determine the total thiol content in the femur tissue, 50 g of homogenized tissue was mixed with 250 μ L of Tris-EDTA and incubated at 25 °C for 10 min. The initial absorbance (α) was recorded at 412 nm using a Stat Fax ELISA reader (Stat Fax, United States). Following this, 20 μ L of DTNB (5,5-dithio-bis-(2-nitrobenzoic acid)) was added, and the mixture was incubated at 25 °C for an additional 20 min. The final absorbance (β) was measured again at 412 nm. The absorbance of a blank solution containing DTNB (μ) was also recorded. The total thiol concentration was then calculated using the formula: Total thiol concentration (μ M) = ($\beta - \alpha - \mu$) \times 1.07 / 6.8 (Shaldoum *et al.*, 2021).

Real-time polymerase chain reaction (real-time PCR) assay

Total RNA extraction. Total RNA was isolated from femur tissue using the Bio Basic animal total RNA purification kit (Bio Basic Inc., Canada) following the manufacturer's instructions. Initially, 50 mg of femur tissue was ground in liquid nitrogen and placed in RNase-Free 1.5 mL centrifuge tubes with 350 μ L of Buffer Rlysis-AG. This mixture was incubated for 5 min at 25 °C, after which 300 μ L of ethanol was added and mixed gently. The mixture was then transferred to a spin column and centrifuged at 12,000 g for 30 s at 25 °C. Subsequently, 0.5 ml each of the kit's GT and NT solutions were added in two separate steps, with centrifugation at 12,000 g for 30 s after each addition. Finally, 50 μ L of RNase-free water was added, incubated for 2 min at 25 °C, and centrifuged at 12,000 g for 30 s. The extracted RNA was stored at -80°C (Yang *et al.*, 2013).

cDNA synthesis and quantitative Real-Time PCR (qPCR). To synthesize cDNA from femur tissue RNA, the Takara cDNA synthesis kit was used following its protocol. A reaction mixture of 1000 ng total RNA, 1 μ L oligo and random primers, 10 μ L Takara Bio Mastermix, and μ mL deionized water was prepared and incubated in a thermal cycler with specific temperature settings: 10 min at 25 °C, 45 min at 60 °C, and 5 min at 60°C. For real-time PCR, the mixture included 1000 ng cDNA, 1 μ L each of forward and reverse primers, and 8 μ L Takara Bio Mastermix, and was run in an Applied Biosystems Quantstudio 1 thermocycler.

PCR cycling consisted of 5 min at 50 °C, 15 s at 95 °C, 1 min at 60 °C, and 5 min at 70°C for 42 cycles, followed by a melting curve analysis from 60-95 °C. CT values for target genes and b-actin were recorded and analyzed with the fold change formula.

$\Delta\Delta CT = [(CT S - Ct_{\beta\text{-actin}}) - (CT S - CT C)]$, Fold change of genes = $2^{-\Delta\Delta CT}$ (Kuang *et al.*, 2019).

Primers were designed using Primer-3 and their specificity was validated through NCBI's blast search. Here are the primer sequences used in the study:

For β -actin, the forward sequence is 5'-CTCTGTGTGGATTGGTGGCT-3', and the reverse sequence is 5'-CGCAGCTCAGTAACAGTCCG-3. The OPG gene uses the forward sequence 5'-TGAGACGTCATCGAAAGCAC-3' and the reverse sequence 5'-CGCACAGGGTGACATCTATT-3. For RANKL, the forward primer is 5'-TTCAGAATTGCCCGACCAGTTTTT-3', and the reverse primer is 5'-CCCAGACATTTGCACACCTCAC-3. The BMP-2 gene's forward sequence is 5'-CAGGAAGCTTTGGGAAACAG-3', with a reverse sequence of 5'-GTCGAAGCTCCCACTGAC-3'. Lastly, for RANK, the forward sequence is 5'-ATCTTCGGCGTTTACTAC-3', and the reverse sequence is 5'-TCCTTATTTCCACTTAGACTAC-3' (Xu *et al.*, 2023).

Femur tissue histopathology. To assess the histopathological changes in femur tissue, the bone samples were dissected and fixed in 10 % formalin. The decalcification process was carried out using 10 % formic acid. Sections of 5 μ m thickness were prepared and mounted on slides. Hematoxylin and eosin staining was performed to examine trabecular thickness, mineralization of spicules, osteoblast density, and bone marrow cell spaces. The analysis was conducted at 100X magnification with an optical microscope (Model No. BX61TRF; Olympus, Japan) and recorded using ImageJ software (Akbari *et al.*, 2017).

Immunohistochemically evolution of bone tissue. The prepared slides, sectioned at 5 μ m thickness, were placed in a microwave with 1X TBS solution (Sigma, USA) and heated at 100 °C for 10 min. The samples were then left in the solution for an additional 20 min. Following this, the samples were subjected to three washes with PBS (Sigma, USA), each for 5 min. Next, a mixture of H₂O₂ (Sigma, USA) and methanol at a 1:9 ratios was applied to the samples for 10 min at 25 °C. After washing with PBS, the primary antibody against p53 (Abcam, USA), diluted 1:100 in PBS, was added and incubated at 25 °C for 60 min. The samples were then washed three times with PBS, followed by the addition of

100 μ L of a linker solution (Diagnostic BioSystems, USA) for 15 min. The samples were washed again three times with PBS and treated with 100 μ L of polymer solution (Diagnostic BioSystems, USA) for 30 min. After another PBS wash, 100 μ L of DAB solution (ScyTek, USA) was applied. After 5 min, the samples were washed with water, then stained with hematoxylin for 1 min, and washed with water once more. Finally, after dehydration and clearing, coverslips were mounted on the samples, which were then photographed using an Olympus CX2 optical microscope connected to a KECAM 5 MP camera system (Velletri *et al.*, 2021).

Statistical analysis. To compare quantitative results across the groups, one-way analysis of variance (ANOVA) followed by the Newman–Keuls post hoc test was employed. A p-value of less than 0.05 was deemed statistically significant. Data normality was assessed using the Kolmogorov-Smirnov test, with p-values above 0.05 indicating normal and homogeneous distributions. Results are presented as means \pm standard deviation (SD). Data analysis was conducted using SPSS software (Version 16; IBM Inc., US), and graphs were created with GraphPad Prism software (Version 9; GraphPad Inc., USA).

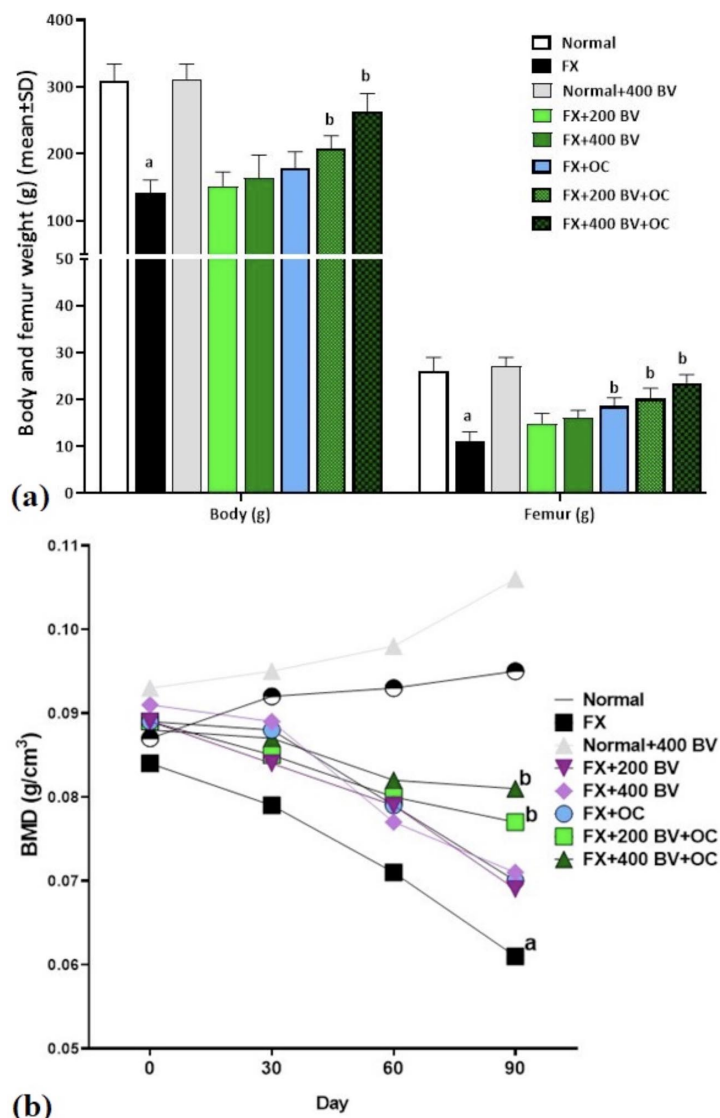


Fig. 2. (a) Mean femur and body weights (g) and (b) Mean femur tissue BMD (g/cm³) by DXA of rats across the normal control, FX, normal+400 BV, FX+200 BV, FX+400 BV, FX+OC, and FX+200 BV+OC and FX+400 BV+OC groups. a (p<0.05) indicates significant differences between FX and normal control groups; b (p<0.05) indicates significant differences between all treated groups and FX group (n = 10 rats/group; values are presented as means \pm SD).

RESULTS

Acute toxicity test (LD₅₀). The LD₅₀ of BV was evaluated by monitoring rats for 24 h, and it was determined that none of the tested doses resulted in mortality. At a dose of 5000 mg/kg, a reduction in appetite was noted, but no other toxic effects were observed at this or lower doses. The highest dose at which no toxic symptoms were detected was 2000 mg/kg. Using Lorke's formula, the LD₅₀ of BV was calculated to be 3.162 g/kg, indicating that doses below 3162 mg/kg are considered safe for rats. However, the safety and potential toxicity of BV may differ among various animal species and humans, necessitating further research to establish safe dosage levels for human use.

Weights of body and femur in rats. The study results revealed a significant reduction in both body weight and femur weight at the end of the study following femur fracture, compared to the normal control group (p < 0.05). However, BV treatment improved these weight parameters. Notably, the co-treatment groups of BV and OC showed significant weight gain, with the FX+200 BV+OC group (p < 0.05) and the FX+400 BV+OC group (p < 0.05) exhibiting greater weight increases compared to the FX group (p < 0.05) (Fig. 2a).

Bone mineral density. The evaluation of bone mineral density (BMD) showed a decrease in all groups of rats with fractured femurs compared to the normal control group. This reduction was significant (p < 0.05) in the FX group. However, on the 90th day of the study, there was a significant increase (p < 0.05) in BMD in the co-treatment groups of BV and OC (FX+200 and 400 BV+OC groups) compared to the FX group (Fig. 2b).

P and Ca serum levels, and ALP activity. Following a femur fracture, there was a notable disruption in Ca-P homeostasis, evidenced by a significant decrease in serum phosphorus and calcium levels compared to the normal control group ($p < 0.05$) and a significant increase in ALP activity ($p < 0.05$). BV treatment helped restore bone mineral balance, with BV alone significantly raising serum calcium levels ($p < 0.05$) and reducing ALP activity ($p < 0.05$)

compared to the FX group. The most pronounced effects were observed in the co-treatment group with OC, particularly in the FX+400 BV+OC group. In these co-treatment groups, there was a significant dose-dependent reduction in ALP activity ($p < 0.05$) and a notable increase in serum calcium and phosphorus levels ($p < 0.05$) compared to the FX group (Fig. 3a).

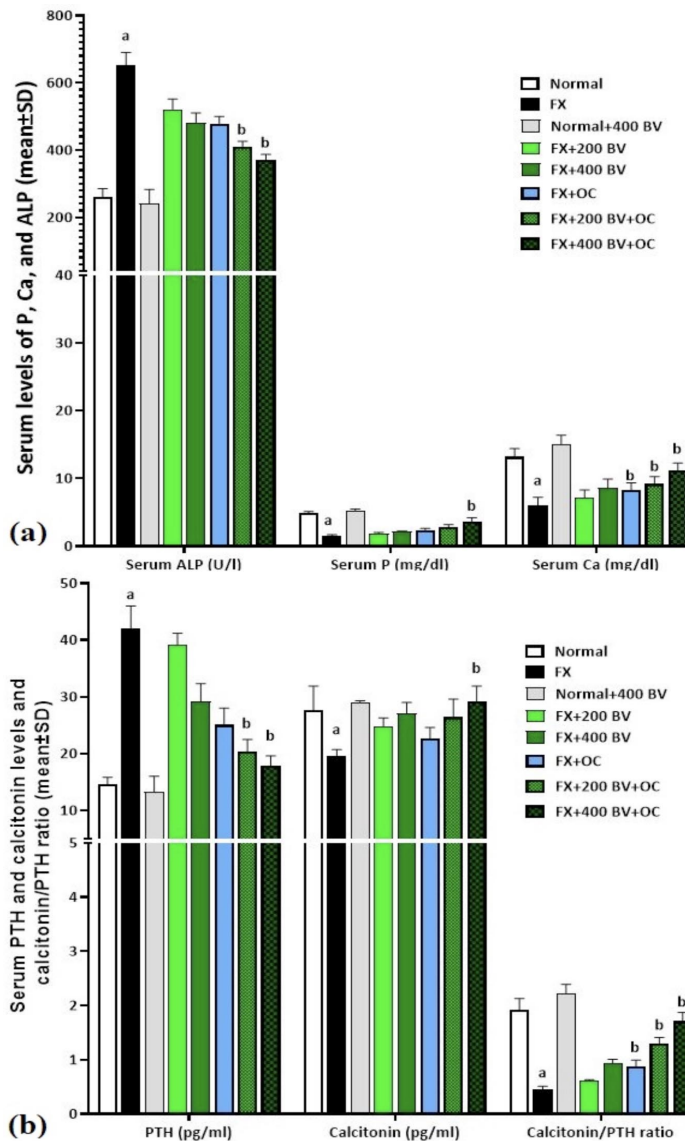


Fig. 3. (a) Mean serum activity of ALP (U/l) along with P and Ca (mg/dl) levels and (b) Mean serum levels of PTH and calcitonin (pg/ml) along with calcitonin/PTH ratio of rats across the normal control, FX, normal+400 BV, FX+200 BV, FX+400 BV, FX+OC, and FX+200 BV+OC and FX+400 BV+OC groups. a ($p < 0.05$) indicates significant differences between FX and normal control groups; b ($p < 0.05$) indicates significant differences between all treated groups and FX group ($n = 10$ rats/group; values are presented as means \pm SD).

PTH and calcitonin serum levels. The analysis of serum hormone levels related to osteogenesis revealed that, in the FX group, PTH levels increased significantly ($p < 0.05$), while calcitonin levels decreased ($p < 0.05$), leading to a reduced calcitonin/PTH ratio ($p < 0.05$) compared to the normal control group. BV alone notably decreased PTH levels ($p < 0.05$) compared to the FX group. In the co-treatment groups (FX+200 BV+OC and FX+400 BV+OC), both BV and OC synergistically and dose-dependently reduced PTH levels significantly ($p < 0.05$) and increased calcitonin levels ($p < 0.05$) compared to the FX group (Fig. 3b).

IL-6, TNF- α , and IL-1 β serum levels. After femur fracture and inflammation, the levels of all three pro-inflammatory cytokines significantly increased ($p < 0.05$) compared to the normal control group. However, BV, with its anti-inflammatory properties, notably reduced ($p < 0.05$) the levels of all three cytokines at a dose of 400 mg/kg compared to the FX group. The greatest reduction in cytokine levels was observed in the synergistic treatment groups combining BV and OC (FX+200 BV+OC and FX+400 BV+OC), where all three cytokines showed a significant decrease ($p < 0.05$) in a dose-dependent manner compared to the FX group (Fig. 4a).

Femur tissue stress oxidative parameters. Following a femur fracture, the TAC (FRAP levels) in the femur significantly decreased ($p < 0.05$) compared to the normal control group, leading to increased lipid peroxidation (indicated by lower TBARS levels) and elevated total thiol levels in the femur tissue ($p < 0.05$). However, BV alone significantly increased FRAP ($p < 0.05$) compared to the FX group, resulting in reduced lipid peroxidation (evidenced by higher TBARS levels) and lower total thiol levels ($p < 0.05$). Improvements in antioxidant parameters were also observed in the BV and OC co-treatment groups (FX+200 BV+OC and FX+400 BV+OC), where, in a dose-dependent and synergistic manner, both FRAP and TBARS levels in the femur tissue increased significantly ($p < 0.05$), and total thiol levels decreased significantly ($p < 0.05$) compared to the FX group (Fig. 4b).

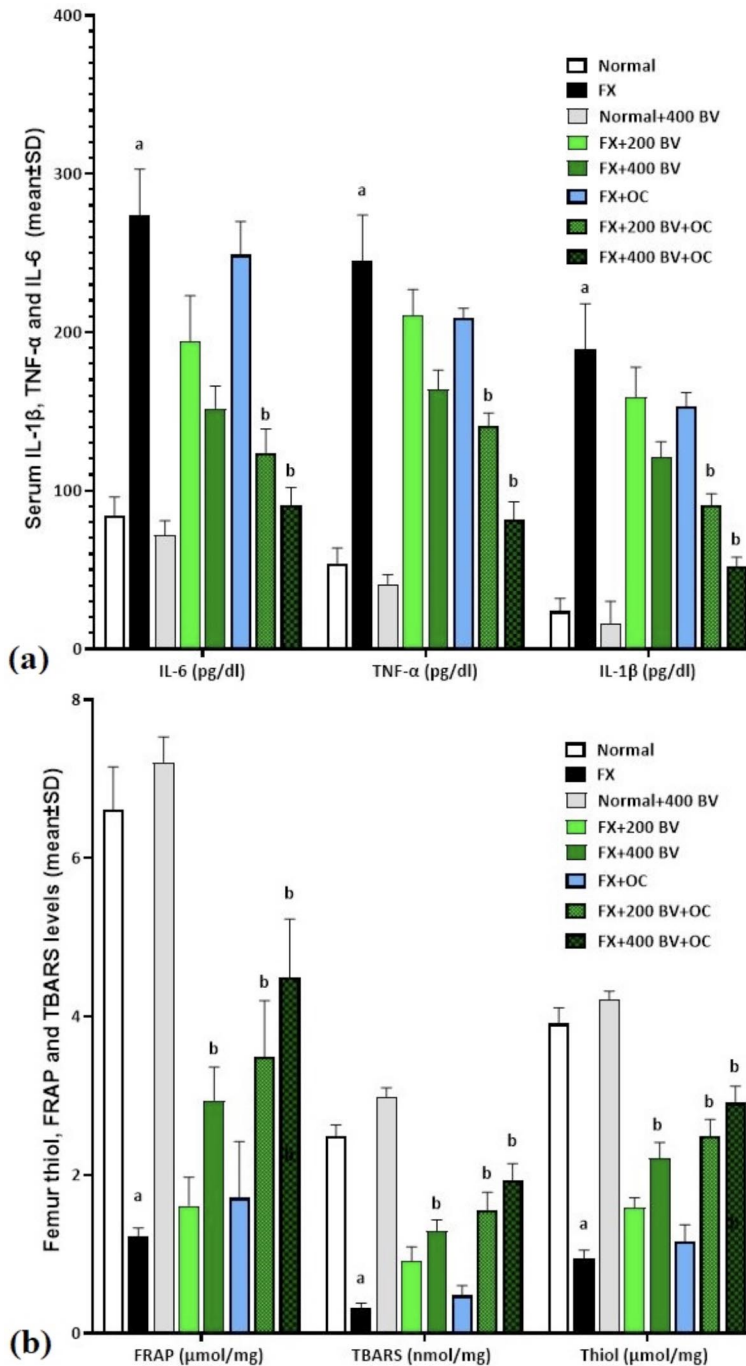


Fig. 4. (a) Mean serum levels of IL-1 β , IL-6, and TNF- α (pg/dL) and (b) Mean femur tissue levels of FRAP (μ mol/mg protein) and TBARS (nmol/mg proteins) of rats across the normal control, FX, normal+400 BV, FX+200 BV, FX+400 BV, FX+OC, and FX+200 BV+OC and FX+400 BV+OC groups. a ($p < 0.05$) indicates significant differences between FX and normal control groups; b ($p < 0.05$) indicates significant differences between all treated groups and FX group ($n = 10$ rats/group; values are presented as means \pm SD).

Expression of RANK, RANK-L, OPG, and BMP-2 genes. Following a femur fracture, osteoclast activity increases, resulting in bone

degradation, with a notable decrease in the expression of RANK, OPG, and BMP-2 genes ($p < 0.05$) and a significant increase in RANK-L gene expression ($p < 0.05$) compared to the normal control group. However, when BV is combined with OC, there is a synergistic improvement in the expression of osteoblast-stimulating genes. In the FX+200 BV+OC group, the expression of RANK and OPG genes significantly increased ($p < 0.05$), while RANK-L expression significantly decreased ($p < 0.05$) compared to the FX group. The most pronounced effect was observed in the FX+400 BV+OC group, where all four genes—RANK, OPG, and BMP-2—showed significant upregulation ($p < 0.05$) compared to the FX group, and RANK-L gene expression significantly decreased ($p < 0.05$) (Fig. 5).

Histopathological findings of the femur tissue. Following a femur fracture, the resulting inflammation, edema, and damage to the endosteum and periosteum can hinder mineralization and the development of spicules and trabeculae in the affected area. This is often accompanied by a lack of new osteon formation by osteoblasts and the presence of fibrous tissue. However, in the groups treated with BV alone and the combined BV and OC treatment, there was evidence of new osteon, trabeculae, and mineral trabeculae formation. The healing regions displayed organized bone islands centered around osteocytes and encircled by osteoblasts, as shown in Figure 6. These results indicate that BV, particularly when combined with OC, can enhance bone repair and foster the formation of new bone tissue, leading to improved healing outcomes.

Expression of femur bone p53. The investigation of p53 gene expression revealed that it was minimal in the normal control group. In contrast, the FX group exhibited significantly elevated levels of p53 expression across various osteogenic areas. Treatment with OC and BV at doses of 200 and 400 mg/kg led to a reduction in p53 expression. This decrease was observed in a dose-dependent manner in trabeculae, osteogenic areas near the endosteum, and hematopoietic islets in the BV-treated groups, particularly when combined with OC (Fig. 7).

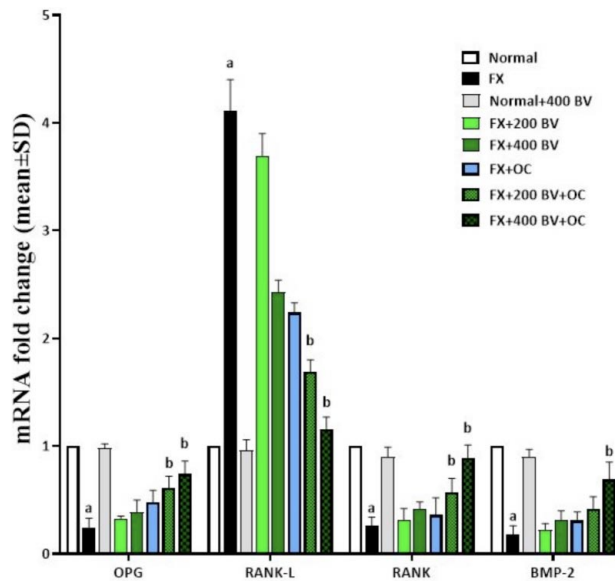


Fig. 5. Mean femur tissue genes expression of RANK, OPG, BMP-2, and RANK-L of rats across the normal control, FX, normal+400 BV, FX+200 BV, FX+400 BV, FX+OC, and FX+200 BV+OC and FX+400 BV+OC groups. a ($p < 0.05$) indicates significant differences between FX and normal control groups; b ($p < 0.05$) indicates significant differences between all treated groups and FX group ($n = 10$ rats/group; values are presented as means \pm SD).

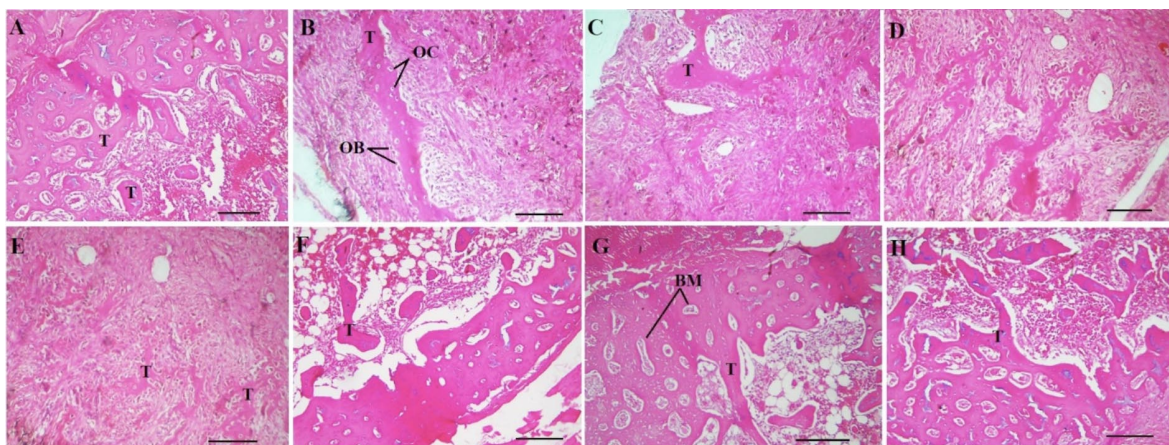


Fig. 6. The femur bone histopathology in normal control (A), FX (B), normal+400 BV (C), FX+200 BV (D) and FX+400 BV (E), FX+OC (F) and FX+200 BV+OC (G) and FX+400 BV+OC (H) groups. (H&E staining $\times 100$, Scale bar = 200 μ m). Osteoblast (OB), osteocyte (OC) cells, bone trabecula (T), bone matrix (BM).

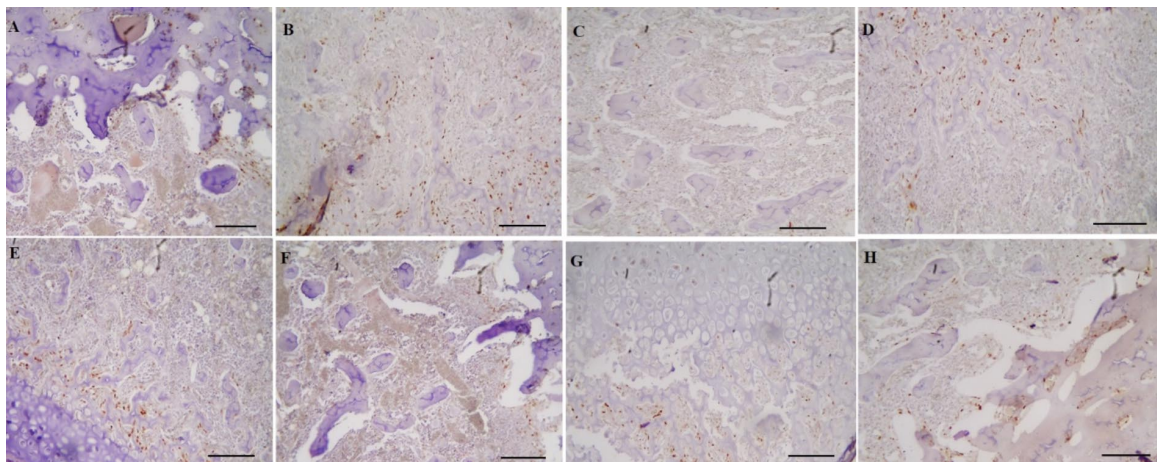


Fig. 7. Immunohistochemical staining of the p53 in femur bone in normal control (A), FX (B), normal+400 BV (C), FX+200 BV (D) and FX+400 BV (E), FX+OC (F) and FX+200 BV+OC (G) and FX+400 BV+OC (H) groups. (DAB staining $\times 100$, Scale bar = 200 μ m).

DISCUSSION

The findings from this study indicate that BV enhances bone healing through several mechanisms. Its substantial mineral content aids in sustaining serum calcium levels within the ideal range (20-30 mg/dL) and boosts the calcitonin/PTH hormone ratio. Additionally, the high polyphenol concentration in BV enhances the OPG/RANK-L ratio, thereby stimulating osteoblast proliferation, differentiation, and activity. BV also helps to mitigate the impact of free radicals, apoptotic pathways, and inflammatory cytokines that could impede bone healing, thereby promoting effective bone repair.

Following a bone fracture, low blood calcium levels (typically falling below 20-30 mg/dL) activate osteoclasts while inhibiting osteoblasts. This imbalance results in an increased PTH/calcitonin ratio and suppression of collagen aggregate formation and matrix vesicle development, which impedes bone repair. This issue is particularly prevalent among individuals with naturally low calcium levels, such as postmenopausal women and elderly men. Research indicates that both chemical and natural supplements containing calcium are beneficial for bone repair by activating osteoblasts and inhibiting osteoclasts (Shuid *et al.*, 2010; Patel *et al.*, 2016). Xu *et al.* (2020), found that calcium plays a crucial role in bone repair by enhancing calcitonin levels, which supports bone healing. Additionally, serum calcium levels affect the OPG/RANK-L pathway and bone metabolism. Low calcium levels are linked to higher RANKL expression and lower OPG expression, leading to increased osteoclast activity and bone resorption. Conversely, higher calcium levels reduce RANKL expression and increase OPG expression, improving bone health by decreasing osteoclast activity (Tobeiha *et al.*, 2020). The study by Soltani *et al.* (2024), demonstrated that BV promotes the differentiation of ovine fetal bone marrow-mesenchymal stem cells into osteocytes. This effect was achieved by increasing the expression of ALP, Runx2, and COL1A2 genes, which in turn stimulated the mineralization of the cell matrix (Soltani *et al.*, 2024). In another study by Xu *et al.* (2020), on glucocorticoid-induced osteoporosis in rats, it was demonstrated that BV enhances biomechanical properties, including bone mineral density (BMD) and trabecular thickness, by inhibiting bone resorption and promoting bone formation (Xu *et al.*, 2020). In this study, BV was found to elevate serum calcium levels and improve the calcitonin/PTH and OPG/RANK-L ratios at both gene and protein levels, thereby enhancing bone healing and increasing bone mineral density (BMD) in BV-treated groups. Furthermore, BV demonstrated synergistic effects with commonly prescribed bone repair medications and supplements, including OC.

Free radicals like H_2O_2 , $\bullet O_2^-$, and $\bullet OH$ are unstable molecules that can inflict oxidative damage on cells and tissues. These radicals are byproducts of normal cellular metabolism but can be produced in greater amounts in response to injury or inflammation. Excessive production of free radicals leads to oxidative stress, which disrupts cellular functions and damages DNA, proteins, and lipids (Wang *et al.*, 2020; Marcucci *et al.*, 2023). Research by Shao *et al.* (2021), has shown that these reactive species can promote mitochondrial apoptosis in osteoprogenitor cells and osteoblasts through the Bax/Caspase-3/p53/Cytochrome C pathway (Shao *et al.*, 2021). Additionally, free radicals can inhibit osteoblast proliferation and differentiation by activating apoptotic signaling pathways, including MAPKs, ERK1/2, and JNK, thus interfering with bone repair processes. They also increase the RANK-L/OPG ratio, which boosts osteoclast activity (Prasadam *et al.*, 2021). Bone fractures trigger a surge of free radicals that overwhelms the tissue's natural antioxidant defenses. Research has also linked the ERK/NF-kB/TNF/IL-6 pathway, which is influenced by free radicals, to osteoclast apoptosis (Herrmann *et al.*, 2011). In this study, bone fractures led to a decrease in endogenous antioxidant enzyme activity and overall antioxidant capacity, accompanied by increased lipid peroxidation due to damage to osteoblastic and osteoprogenitor cell membranes. The presence of polyphenolic compounds in BV, such as apigenin, genistein, kaempferol, quercetin, and formononetin, appears to boost the antioxidant defense system and improve markers of oxidative stress in serum and tissues. Rafiee *et al.* (2016), demonstrated that BV offered protection to the testes from the harmful effects of carbon tetrachloride in Wistar rats (Rafiee *et al.*, 2016). This protective effect was attributed to the increased antioxidant activity of serum catalase (CAT) and a reduction in malondialdehyde (MDA) levels in testicular tissue, which helped preserve the testes' structure and function (Rafiee *et al.*, 2016). Similarly, Sonei *et al.* (2020), found that barberry extract had a protective effect on mouse brain tissue exposed to the toxic substance diazinon. The extract enhanced the activity of antioxidant enzymes such as glutathione peroxidase (GPx), glutathione (GSH), superoxide dismutase (SOD), and catalase (CAT), resulting in improved behavioral performance and better brain structure (Sonei *et al.*, 2020).

Isoflavones like genistein, formononetin, and biochanin A can inhibit osteoclast differentiation and activity through the ERK, p38, and AKT signaling pathways. These isoflavones help to reduce the RANK-L/OPG ratio by enhancing the RANK/OPG system, ultimately boosting the proliferation, activity, and differentiation of osteoblasts (Cepeda *et al.*, 2020). Additionally, research has shown that pro-inflammatory cytokines such as $TNF\alpha$, IL-1, IL-6, IL-

7, and IL-17 increase during bone damage. These cytokines hinder the OPG/RANK/BMP-2 and BMP-2/Smad/Wnt signaling pathways, leading to enhanced osteoclastogenesis and suppressed osteoblast differentiation (Wu & Liu, 2022). Specifically, IL-6 functions as an inhibitor of BMP-2 or the OPG/RANKL pathway, disrupting osteoblast activity. In the current study, levels of pro-inflammatory cytokines rose following bone fracture, but BV was effective in regulating these cytokines due to its polyphenolic content, thereby supporting osteogenesis (Sahin *et al.*, 2021; Arafa *et al.*, 2023). Based on these findings, BV appears to be a promising option for treating bone fractures and even for preventing fractures in at-risk groups, such as the elderly, individuals with low serum calcium levels, postmenopausal women, and those with absorption disorders. In such cases, BV could be used alongside calcium supplementation to enhance bone health.

CONCLUSION

The study's findings suggest that BV can enhance bone density and expedite bone repair, especially in individuals with fractures, by modulating antioxidant and anti-inflammatory pathways, regulating crucial minerals for bone healing, and reinforcing the OPG/RANK/BMP-2 pathway. Consequently, BV could serve as a preventive measure for those at risk of fractures. Moreover, BV may be beneficial for individuals with fractures to aid in bone healing and improve overall bone health. Further research is recommended to explore additional signaling pathways influenced by BV in bone repair, as well as to evaluate its effects in other in-vivo and in-vitro models. Future studies may also consider developing a prodrug containing the pure extract or active components of BV.

Conflict of interest. The authors declare that there is no conflict of interest.

Ethical approval. The experimental protocols of this study were approved by Xi'an International Medical Center Hospital.

BAI, J. & LIANG, Q. Mejora de la mineralización ósea y la actividad osteoprogenitora por *Berberis vulgaris* L.: perspectivas sobre la modulación de la vía BMP-2 y RANK en un modelo de fractura de fémur de rata. *Int. J. Morphol.*, 43(1):258-268, 2025.

RESUMEN: *Berberis vulgaris* L. (BV) es rico en isoflavonoides y minerales esenciales que pueden mejorar la reparación ósea al promover la diferenciación de osteoblastos, estimular osteoprogenitores e inhibir la actividad de los osteoclastos. Este estudio exploró los efectos

del extracto de BV en la curación ósea utilizando un modelo de fractura de fémur en ratas Wistar. Se dividieron ochenta ratas en ocho grupos, incluido un control normal que recibió agua destilada (DS), un grupo tratado con BV que recibió 200 mg/kg de BV diariamente, un grupo con fractura tratado con DW y grupos con fractura que recibieron 200 o 400 mg/kg de BV diariamente. Además, a un grupo de fracturas se le administró jarabe Osteocare (OC), mientras que dos grupos combinados recibieron BV con jarabe OC. Se realizaron evaluaciones radiográficas de fracturas de fémur y densidad mineral ósea (DMO) a los 30, 60 y 90 días mediante absorciometría de rayos X de energía dual (DXA). Se midieron los niveles séricos de calcio, fósforo y fosfatasa alcalina (ALP), junto con calcitonina y hormona paratiroidea (PTH) utilizando kits ELISA. El tejido óseo se analizó para la expresión del gen p53 a través de inmunohistoquímica, y se evaluó la estimulación osteoprogenitora midiendo la expresión de los genes OPG, RANK, RANKL y BMP-2. Los resultados indicaron que la suplementación con BV mejoró significativamente la DMO y los niveles séricos de marcadores de formación ósea y hormonas relacionadas con la osteogénesis. El estudio sugiere que BV influye positivamente en la curación ósea a través de la modulación de la vía OPG/RANK/BMP-2 y puede ser un agente terapéutico prometedor para la curación de fracturas y el tratamiento de la osteoporosis.

PALABRAS CLAVE: Osteogénesis; Densidad mineral ósea; Cicatrización ósea; *Berberis vulgaris* L.; Fractura de fémur.

REFERENCES

- Akbari, M.; Goodarzi, N. & Tavafi, M. Stereological assessment of normal Persian squirrels (*Sciurus anomalus*) kidney. *Anat. Sci. Int.*, 92:267-74, 2017.
- Arafa, E. A.; Elgendy, N. O.; Elhemely, M. A.; Abdelaleem, E. A. & Mohamed, W. R. Diosmin mitigates dexamethasone-induced osteoporosis in vivo: Role of Runx2, RANKL/OPG, and oxidative stress. *Biomed. Pharmacother.*, 161:114461, 2023.
- Azizieh, F. Y.; Shehab, D.; Jarallah, K. A.; Gupta, R. & Raghupathy, R. Circulatory levels of RANKL, OPG, and oxidative stress markers in postmenopausal women with normal or low bone mineral density. *Biomarker Insights*, 14:1177271919843825, 2019.
- Babic Leko, M.; Pleic, N.; Gunjaca, I. & Zemunik, T. Environmental factors that affect parathyroid hormone and calcitonin levels. *Int. J. Mol. Sci.*, 23(1):44, 2021.
- Cepeda, S. B.; Sandoval, M. J.; Crescitelli, M. C.; Rauschemberger, M. B. & Massheimer, V. L. The isoflavone genistein enhances osteoblastogenesis: Signaling pathways involved. *J. Physiol. Biochem.*, 76(1):99-110, 2020.
- Goodman S. B.; Pajarinen J.; Yao Z. & Lin T. Inflammation and bone repair: from particle disease to tissue regeneration. *Front. Bioeng. Biotechnol.*, 19:7:230, 2019.
- Herrmann J. L.; Weil B. R.; Abarbanell A.M.; Wang Y.; Poynter J. A.; Manukyan M. C., & Meldrum DR. IL-6 and TGF- α costimulate mesenchymal stem cell vascular endothelial growth factor production by ERK-, JNK-, and PI3K-mediated mechanisms. *Shock*. 35(5):512-6, 2011.

- Houschyar, K. S.; Tapking, C.; Borrelli, M. R.; Popp, D.; Duscher, D.; Maan, Z. N.; Chelliah, M. P.; Li, J.; Harati, K.; Wallner, C.; Rein, S.; Pfföringer, D.; Reumuth, G.; Grieb, G.; Mouraret, S.; Dadras, M.; Wagner, J. M.; Cha, J. Y.; Siemers, F.; Lehnhardt, M. & Behr, B. Wnt pathway in bone repair and regeneration—what do we know so far. *Front. Cell. Dev. Biol.*, 6:170, 2020.
- John-Africa L. B. Studies on the acute toxicity of the aqueous extract of *Alysicarpus ovalifolius* in mice. *Sci. World J.*, 14(1):43-6, 2019.
- Kobayashi, K.; Nojiri, H.; Saita, Y.; Morikawa, D.; Ozawa, Y.; Watanabe, K. & Shimizu, T. Mitochondrial superoxide in osteocytes perturbs canalicular networks in the setting of age-related osteoporosis. *Sci. Rep.*, 5(1):9148, 2015.
- Kuang, M. J.; Xing, F.; Wang, D.; Sun, L.; Ma, J. X., & Ma, X. L. CircUSP45 inhibited osteogenesis in glucocorticoid-induced osteonecrosis of femoral head by sponging miR-127-5p through PTEN/AKT signal pathway: experimental studies. *Biochem. Biophys. Res. Commun.*, 509(1):255-61, 2019.
- Lv, W. T.; Du, D. H.; Gao, R. J.; Yu, C. W.; Jia, Y.; Jia, Z. F & Wang C. J. Regulation of hedgehog signaling offers a novel perspective for bone homeostasis disorder treatment. *Int. J. Mol. Sci.*, 20(16):3981, 2019.
- Marcucci, G.; Domazetovic, V.; Nediani, C.; Ruzzolini, J.; Favre, C. & Brandi, M. L. Oxidative stress and natural antioxidants in osteoporosis: Novel preventive and therapeutic approaches. *Antioxidants*, 12(2):373, 2023.
- Patel, L.; Bernard, L. M. & Elder, G. J. Sevelamer versus calcium-based binders for treatment of hyperphosphatemia in CKD: a meta-analysis of randomized controlled trials. *Clin. J. Am. Soc. Nephrol.*, 11(2):232-44, 2016.
- Patidar, V.; Shah, S.; Kumar, R.; Singh, P. K.; Singh, S. B. & Khatri, D. K. A molecular insight of inflammatory cascades in rheumatoid arthritis and anti-arthritic potential of phytoconstituents. *Mol. Biol. Rep.*, 49(3):2375-91, 2022.
- Prasadam, I.; Friis, T.; Shi, W.; van Gennip, S.; Crawford, R. & Xiao Y. Osteoarthritic cartilage chondrocytes alter subchondral bone osteoblast differentiation via MAPK signalling pathway involving ERK1/2. *Bone*, 46(1):226-35, 2021.
- Rafiee, F.; Nejati, V.; Heidari, R. & Ashraf, H. Protective effect of methanolic extract of *Berberis integerrima* Bunge. root on carbon tetrachloride-induced testicular injury in Wistar rats. *Int. J. Reprod. Biomed.*, 14(2):133-40, 2016.
- Rahimi-Madiseh, M.; Lorigoini, Z.; Zamani-Gharaghoshi, H. & Rafieian-Kopaei, M. *Berberis vulgaris*: specifications and traditional uses. *Iran. J. Basic Med. Sci.*, 20(5):569-87, 2017.
- Sahin, E.; Orhan, C.; Balci, T. A.; Erten, F. & Sahin, K. Magnesium picolinate improves bone formation by regulation of RANK/RANKL/OPG and BMP-2/Runx2 signaling pathways in high-fat fed rats. *Nutrients*, 13(10):3353, 2021.
- Shaldoum, F.; El-kott, A. F.; Ouda, M. M. & Abd-Ella, E. M. Immunomodulatory effects of bee pollen on doxorubicin-induced bone marrow/spleen immunosuppression in rat. *J. Food Biochem.*, 45(6):e13747, 2021.
- Shao, J.; Liu, S.; Zheng, X.; Chen, J.; Li, L. & Zhu, Z. Berberine promotes peri-implant osteogenesis in diabetic rats by ROS-mediated IRS-1 pathway. *BioFactor*, 47(1):80-92, 2021.
- Shuid, A. N.; Mohamad, S.; Mohamed, N.; Fadzilah, F. M.; Mokhtar, S. A.; Abdullah, S.; Othman, F.; Suhaimi, F.; Muhammad, N. & Soelaiman, I. N. Effects of calcium supplements on fracture healing in a rat osteoporotic model. *J. Orthop. Res.* 28(12):1651-6, 2010.
- Soltani, L.; Ghaneialvar, H.; Abbasi, N.; Bayat, P. & Nazari, M. Chitosan/alginate scaffold enhanced with *Berberis vulgaris* extract for osteocyte differentiation of ovine fetal stem cells. *Cell. Biochem. Funct.*, 42(1):e3924, 2024.
- Sonei, A.; Fazelipour, S.; Kanaani, L. & Jahromy, M. H. Protective effects of *Berberis vulgaris* on diazinon-induced brain damage in young male mice. *Prev. Nutr. Food Sci.*, 25(1):65-70, 2020.
- Sun Y., Xu L., Huang S., Hou Y., Liu Y., Chan K. M., Pan X., & H, Li G (2015). mir-21 overexpressing mesenchymal stem cells accelerate fracture healing in a rat closed femur fracture model. *Biomed. Res. Int.*, 2015:412327, 2015.
- Tobeiha, M.; Moghadasian, M. H.; Amin, N. & Jafarnejad, S. RANKL/RANK/OPG pathway: a mechanism involved in exercise-induced bone remodeling. *Biomed. Res. Int.*, 2020:6910312, 2020.
- Velletri, T.; Huang, Y.; Wang, Y.; Li, Q.; Hu, M.; Xie, N. & Wang, Y. Loss of p53 in mesenchymal stem cells promotes alteration of bone remodeling through negative regulation of osteoprotegerin. *Cell Death Differ.*, 28(1):156-69, 2021.
- Wang, T. & He, C. TNF- α and IL-6: the link between immune and bone system. *Curr. Drug Targets*, 21(3):213-27, 2020.
- Wong, S. K.; Chin, K. Y.; Suhaimi, F. H.; Ahmad, F. & Ima-Nirwana, S. Effects of metabolic syndrome on bone mineral density, histomorphometry and remodelling markers in male rats. *PLoS One*, 13(2):e0192416, 2018.
- Wu, Z. & Liu, L. The protective activity of genistein against bone and cartilage diseases. *Front. Pharmacol.*, 13:1016981, 2022.
- Wu, D.; Li, L.; Wen, Z. & Wang, G. Romosozumab in osteoporosis: yesterday, today and tomorrow. *J. Transl. Med.*, 21(1):668, 2023.
- Xie, J.; Guo, J.; Kanwal, Z.; Wu, M.; Lv, X.; Ibrahim, N. A.; Li, P.; Buabeid, M. A.; Arafa, E. S. & Sun, Q. Calcitonin and bone physiology: in vitro, in vivo, and clinical investigations. *Int. J. Endocrinol.*, 2020:3236828, 2020.
- Xu, J.; Wang, J.; Chen, X.; Li, Y.; Mi, J. & Qin, L. The effects of calcitonin gene-related peptide on bone homeostasis and regeneration. *Curr. Osteoporos. Rep.*, 18(6):621-32, 2020.
- Xu, C.; He, Z. & Shen, Z. Euxanthone Suppresses the Proliferation, Migration and Invasion of Human Medulloblastoma Cells by Inhibiting the RANK/RANKL Pathway. *Pharmacogn. Mag.*, 19(1):23-30, 2023.
- Xue, J. Y.; Ikegawa, S. & Guo, L. Genetic disorders associated with the RANKL/OPG/RANK pathway. *J. Bone Miner. Metab.*, 39(1):45-53, 2021.
- Yang, D.; Yang, W.; Zhang, Q.; Hu, Y.; Bao, L. & Damirin, A. Migration of gastric cancer cells in response to lysophosphatidic acid is mediated by LPA receptor 2. *Oncol. Lett.*, 5(3):1048-52, 2013.
- Zhang, Y.; Liang, J.; Liu, P.; Wang, Q.; Liu L. & Zhao, H. The RANK/RANKL/OPG system and tumor bone metastasis: Potential mechanisms and therapeutic strategies. *Front. Endocrinol. (Lausanne)*, 13:1063815, 2022.
- Zhang, R. H.; Zhang, X. B.; Lu, Y. B.; Hu, Y. C.; Chen, X. Y.; Yu, D. C. & Zhou, H. Y. Calcitonin gene-related peptide and brain-derived serotonin are related to bone loss in ovariectomized rats. *Brain Res. Bull.*, 176:85-92, 2021.
- Zhao, L.; Li, M. & Sun, H. Effects of dietary calcium to available phosphorus ratios on bone metabolism and osteoclast activity of the OPG/RANK/RANKL signalling pathway in piglets. *J. Anim. Physiol. Anim. Nutr.*, 103(4):1224-32, 2019.

Corresponding Author:

Dr. Qingfu Liang

Department of Orthopaedics

Xi'an International Medical Center Hospital

Xi'an, Shaanxi, 710100

CHINA

E-mail: liangqingfu0920@sina.com

Orcid ID Qingfu Liang: 0009-0003-8532-1590